Desalination and Water Treatment
www.deswater.com

doi: 10.5004/dwt.2021.26796

216 (2021) 140–150
March

Solar driven photocatalytic degradation of organic pollutants via Bi_2O_3@reduced graphene oxide nanocomposite

Sadia Iqbal[a], Maria Iqbal[a], Aqsa Sibtain[a], Atia Iqbal[b], Zahoor H. Farooqi[c], Sajjad Ahmad[d], Kiran Mustafa[a], Sara Musaddiq[a,*]

[a]*Department of Chemistry, Kutchery Campus, The Women University Multan, Multan 60000, Pakistan, emails: drsara.chem@wum.edu.pk (S. Musaddiq), sadia.iqbalshahid@gmail.com (S. Iqbal), mariaiqbal089@gmail.com (M. Iqbal), aqsa.sibtain214@gmail.com (A. Sibtain), kiranmustafa100@gmail.com (K. Mustafa)*
[b]*Department of Microbiology and Molecular Genetics, Kutchery Campus, The Women University Multan, Multan 60000, Pakistan, email: atiaiqbal01@gmail.com*
[c]*Institute of Chemistry, University of the Punjab, New Campus, Lahore 54590, Pakistan, email: Zahoor.chem@pu.edu.pk*
[d]*Pakistan Council of Research in Water Resources, Ministry of Science and Technology, Islamabad, Pakistan, email: chsajjadahmad@hotmail.com*

Received 8 February 2020; Accepted 7 November 2020

ABSTRACT

A one-step, simple preparation of plant extract mediated reduced graphene oxide nanocomposite (Bi_2O_3@RGO) is performed by using an aqueous extract of flowers of *Aerva javanica*. The reduction of metal and graphene oxide for nanocomposite preparation is done in a single step where the metabolites present in *A. javanica* played a significant role as reducing and stabilizing agents to prevent agglomeration. UV/Vis, X-ray diffraction, and Fourier transform infrared analysis confirmed the anchoring of bismuth oxide nanoparticles on RGO sheets with an average particle size of 12 nm calculated by Scherrer's formula. The as-prepared nanocomposite displayed significant potential as photocatalyst in solar-driven photodegradation of industrial dyes, that is, Alizarin yellow (Al-Y), Methylene blue (MB), and Lissamine green (LG). The results indicated that 25 mg of synthesized material was able to perform 32.51%, 41.50%, and 52.89% degradation of Lissamine green, Alizarin yellow, and Methylene blue, respectively, in 1.5–2 h using sunlight irradiation. Bi_2O_3@RGO is found more efficient for the photodegradation of MB and photo-degradation of all dyes obeyed pseudo-first-order kinetics. Furthermore, this work was encouraging, as plants extract mediated nanocomposite was found to be useful in mg amount for environmental protection applications.

Keywords: Aerva javanica; Flowers; Aqueous extract; Azo dyes; Photocatalysis; Nanocomposites

1. Introduction

Rapid growth of industries is the leading cause of water pollution as industries are persistently releasing poisonous waste to the water bodies [1]. Organic dyes, frequently employed in textile industries, are major sources of water pollution. These dyes are poisonous and creates severe problems for aquatic life along with the human beings and their removal is very difficult as they are non-biodegradable [2]. A class of the organic dyes known as Azo dyes containing azo group (–N=N–) in their structure, are responsible for coloring a vast variety of articles such as leather, carpets, and cloths. About 10%–50% of these dyes remain unreacted when released in water and

* Corresponding author.

are scientifically proven to be highly carcinogenic and poisonous [3]. In order to ensure the safety of the environment, the disposal of the dyes is of utmost importance.

Several methods have been adapted for the eradication of the dyes from different water bodies. In the recent years' photocatalysis has been frequently researched for the mitigation of water pollution due to its economical and environment friendly nature [4]. Photocatalysis is the process in which solar energy is harnessed by group of the substances and utilized for various processes, for example, water purification technologies [5], for the removal of bacteria and various other organic pollutants [6]. The method of photocatalysis utilizes catalysts along with light to support a chemical reaction. Generally, semiconductors fill in as a facilitator because when photons with greater band gap energy than that of semiconductor's attack the semiconductor substance, the electrons of valence band transfer to the conduction band generating electron–hole pairs. These pairs start redox reactions, where progressive reduction and oxidation reactions are finished by these electrons and holes. Photocatalysis mainly relies upon the catalyst size, where small size attracts large number of atoms toward the surface due to enhanced surface area to volume ratio [7]. Metal nanoparticles and their nanocomposites have been used as efficient heterogeneous photo-catalysts for the management of polluted water owing to large surface area [8]. To establish environment-friendly synthetic procedures for metallic NPs preparation by means of various biological materials, plant extracts have gained much attention as reducing as well as stabilizing agents due to their inexpensive and comparatively handy nature [9]. In plant extracts, the biogenic reducing agents comprising the water-soluble plant metabolites, for example, flavonoids, alkaloids, terpenoids, phenolic compounds, and co-enzymes are found that reduce metal ions to nano sized particles by one-step green synthesis method [10]. Joseph and Mathew [11] reported the microwave aided green synthesis of gold and silver nano catalysts by using leaf extract of *A. lanata* as a stabilizing and reducing agent. They checked the catalytic activity of freshly prepared nanocomposites against $NaBH_4$ assisted reduction of 4-nitrophenol to 4-aminophenol. They observed that gold and silver nano catalysts have shown excellent reduction ability towards reductive degradation of 4-nitrophenol [11].

Bismuth oxide nanocomposites are getting significant attention as promising photocatalysts owing to their relatively narrow band gaps [4]. These nanocomposites have some disadvantages, for example, they exhibit small surface area for the attachment of substrate molecules and recombination of the photo-generated electrons and holes [12], that cause reduction in their practical application as efficient photocatalysts. In order to eliminate these issues and to improve the efficiency of bismuth-based nanocomposites, various approaches have been utilized including different carbon-based materials, employed as a support material, to synthesize bismuth oxide nanocomposites.

Various carbon-based supporting materials exist, for example, carbon nanotubes, carbon dots [13], graphene, graphene oxide (GO), etc. Among these materials' graphene oxide is a remarkable substrate for preparation of metal oxide nanocomposites for water decontamination in visible and ultraviolet lights [14] owing to their unique properties such as fast electron mobility, high conductivity, and greater surface area [15]. Composite substances comprising of GO and RGO (reduced GO) are frequently used for the removal of contamination and dyes from polluted water [16]. Although their photocatalytic activity is somewhat lower on account of wide band gap, however, a mixture of graphene and metal oxide nanoparticles is very helpful in reducing the gap between the bands. One such attempt was made by Safardoust-Hojaghan et al. who prepared and employed N-GQDs/TiO_2 nanocomposites for photodegradation of MB and confirmed that by addition of N-doped graphene QDs to TiO_2 NPs, photodegradation efficiency enhanced from 40% to 85% as compared with pure TiO_2 [17].

Current study is centered on the way to control and oversee the properties of reduced graphene oxide (RGO) by fastening bismuth oxide nanoparticles for photocatalytic degradation of organic pollutants. Some reports are accessible on bismuth semimetal-based nanocomposites, for example, Bi_2O_3/RGO nanocomposite fabrication was reported by chemical oxidation of graphite into graphene oxide followed by a solvothermal method and has been utilized to check the degradation of a model organic dye molecule Methylene blue (MB) [18]. Das et al. [19], reported the synthesis of Bi_2O_3@GO nanocomposite by sonochemical method and this nanocomposite was employed for adsorption and removal of RhB (cationic organic dyes) from industrial wastewater. They studied the effect of different parameters such as temperature, contact time, pH, and amount of adsorbent on the adsorption potential. The percentage removal for the photo-degradation of RhB by utilizing GO and Bi_2O_3@GO was found 64% and 80.7%, respectively [19]. The multi-component nanocomposite of RGO stacked with Bi_2WO_6/Bi_2O_3, prepared by the solvothermal method has been applied for photocatalytic degradation of RhB [20], Bi_2WO_6-RGO nanocomposites have been synthesized by hydrothermal technology and used for photocatalytic decomposition of ecological contaminant bisphenol A, Cr(VI) and benzyl alcohol, a similar material has likewise been utilized for the decomposition of 4-nitrophenol. Rajagopal et al. [21] investigated the photocatalytic ability of Bi_2WO_6-rGO nanocomposite against the degradation of rhodamine B with excellent results. They improved the catalytic potential of the catalyst by enhancing their surface area and reducing the recombining ability of electron and holes by introduction of rGO.

In another attempt, the photocatalytic activity of β-Bi_2O_3/graphene nanocomposite was evaluated by degrading Methylene blue as a model reaction under visible light irradiation where nanocomposites showed enhanced photocatalytic activity as compared to bare β-Bi_2O_3 nanoparticles [22]. The fabrication of nanocomposite consisting of $BiVO_4$, Ag, and rGO was reported and its catalytic ability was evaluated to degrade rhodamine B dye. As compared to the bare $BiVO_4$ and $BiVO_4$-rGO nanocomposite, the prepared composite showed increased visible light activity and higher degradation efficiency of rhodamine B dye [23].

So far, no effort has been made to fabricate photocatalytic Bi_2O_3@RGO nanocomposites by green techniques. An endeavor was made to get Bi_2O_3@RGO by utilizing aq. concentrate of flowers of *Aerva javanica*, a medicinal

plant of genus *Aerva* and Amaranthaceae family (Fig. 2). *A. Javanica* is known to be enriched with flavonoids [24], polyphenolics, and sugars [25]. In the current study, the plant effectively contributed to a single-step reduction of graphene oxide and metal. The prepared nanocomposite displayed promising photocatalytic activity towards Alazarine yellow, Methylene blue, and Lissamine green dyes under sunlight. To the best of our knowledge, photocatalytic degradation of the above-mentioned dyes by using PM-Bi_2O_3@RGO is not reported in the literature.

2. Experimental

2.1. Materials

For the preparation of plant-mediated Bi_2O_3@RGO nanocomposite, graphite powder (C, 99.9%), sulfuric acid (H_2SO_4, 99.99%,), bismuth chloride ($BiCl_3$, ≥98%), and potassium permanganate ($KMnO_4$, ≥99%) were purchased from Sigma Aldrich, Germany. Other reagents such as sodium nitrate ($NaNO_3$, >99%) were purchased from Bio World and hydrogen peroxide (H_2O_2, 3 wt.%) was acquired from Duskan Reagents, Korea. For all solution preparations deionized water was utilized.

2.2. Fabrication of RGO

Flowers of *A. javanica* were obtained from desert area of Pakistan (Cholistan). The flowers were dried in shade; 10 g of flowers were soaked into 100 mL de-ionized water and heated with a magnetic stirrer for 1 h not exceeding the 45°C–50°C. After cooling at room temperature, the concentrate was filtered and centrifuged for the removal of suspended particles. Afterwards, it was stored at 4°C.

In the current study, Hummers procedure [26] was employed with little modifications for the preparation of graphite oxide from graphite. At first, graphite (powder) and sodium nitrate were taken in three neck flask and sulfuric acid was added to the mixture and stirred in ice-cold water. Afterwards 9 g of $KMnO_4$ was added gradually with continuous stirring for 5 d. 200 mL of 5% by wt. sulfuric acid was added to the mixture and it was stirred for 2 h. Later on, an aqueous solution of H_2O_2 was added and the mix was agitated for another 2 h. The mixture was washed afterwards with 3% sulfuric acid and 0.5% hydrogen peroxide. Additionally, the mixture was washed with deionized water. After washing the dispersion was centrifuged at 9,000 rpm for 2 h in deionized water. Finally, it was washed again with de-ionized water several times and

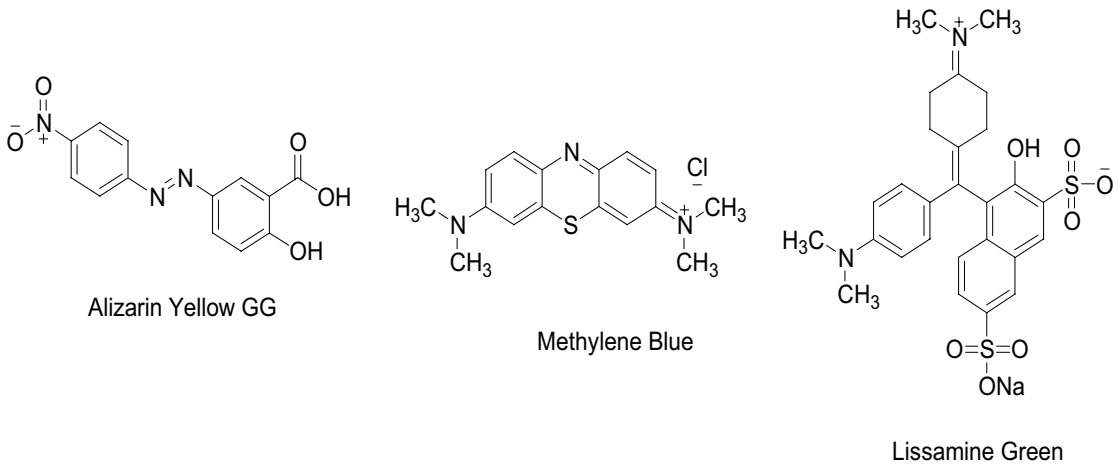

Fig. 1. Structures of dyes used as model pollutants in degradation experiment.

Fig. 2. (a) Flowers and (b) plant of *Aerva javanica*.

brown-black dispersion of graphite oxide was obtained. It is a consecutive procedure in which graphene oxide is made from graphite oxide. The initial stage involves the distribution of graphite oxide in distilled water. Secondly, the mix was allowed to sonicate for 30 min. Later on, aqueous plant extract (density = 0.1 g mL^{-1}) was added in it and the whole dispersion was allowed to stir at 98°C for a day. Dark powdered rGO was obtained as the product. It was washed for many times with distilled water so as to eliminate unnecessary plant concentrate. It was re-dispersed in water by sonication. The final product was collected after centrifugation of the mixture for 30 min at 4,000 rpm.

2.3. Fabrication of plant-mediated Bi_2O_3@RGO

Nanocomposite were prepared by using the reported protocol [8]. $BiCl_3$ and RGO were used for manufacturing of plant-mediated nanocomposite, that is, PM-Bi_2O_3@RGO. RGO dispersion in water was made via sonication. This highly rGO suspension and aqueous extract of *A. javanica* was added along with 0.5 mM of $BiCl_3$ and the mixture was stirred at 90°C for a day. The reaction was halted after 24 h and resulting product was washed and centrifuged at 12,000 rpm and was dried at 80°C, as a result, the black powdery product was obtained. An attempt was also made by synthesizing bismuth oxide nanoparticles separately and then utilizing them for nanocomposite fabrication with rGO.

2.4. Photocatalytic activity of PM-Bi_2O_3@RGO

Photocatalytic degradation of dyes (Al-Y, MB, LG) was monitored by a UV-visible spectrophotometer. To carry out experiments, 25 mg of PM-Bi_2O_3@RGO photocatalyst and 20 mL of 1 ppm aqueous solution of dye was taken in a vial and kept under sunlight with constant stirring. After constant time interval 2 mL of reaction mixture was added to the cuvette, and the spectra were scanned within a range of 200–800 nm using HALO DB-20 (double beam spectrophotometer).

2.5. Characterization

Fourier transform infrared (FTIR) spectra were recorded by using ALPHA (PLATINIUM-ATR) FTIR-spectrometer having range 375–4,000 cm^{-1} with 4 cm^{-1} resolution. UV-visible spectra were scanned by using HALO DB-20 (double beam spectrophotometer) within a range of 200–800 nm. Photocatalytic activity of PM-Bi_2O_3@RGO was also monitored by using HALO DB-20 (double beam spectrophotometer). X-ray diffraction (XRD) pattern of prepared materials was taken through XPERT PRO XRD diffractometer (PANalytical, UK). Cu kα (154 Å) and Mo kα (0.71 Å) are used as source of X-ray in this diffractometer and θ varies 5°–80°.

3. Results and discussion

The efficacious development of RGO and Bi_2O_3@RGO nanocomposites was determined by FTIR, UV-vis absorption spectrophotometer, and XRD analysis. UV-Vis analysis was done to determine the electronic absorption of RGO and intermediates prepared by the extract of the plant. Graphite oxide was synthesized by the oxidizing graphite powder via adjusted Hummers procedure [26] and afterwards, the graphene oxide (GO) sheets were made by sonication [27]. UV-Vis analysis of all products and intermediates was made via their dispersion in water. Fig. 3a depicts the UV-Vis graph of GO dispersion in water, GO showed two absorption peaks (λ_{max}) at 305 nm (C=O) and 228 nm (C=C). After the reduction of the oxide, the C=O absorption peak vanishes and C=C absorption peak is noted at 240 nm (Fig. 3b) [28]. Absorption bands of Bi_2O_3@RGO nanocomposite were observed at 211, 254, and 350 nm with a shoulder at 445 nm. As discussed in experimental section that bismuth oxide nanocomposite was prepared via two methods, in the first method reduction of metal ion and graphene oxide occurred in single step while in second method Bi_2O_3 nanoparticles were prepared first and then utilized for nanocomposite fabrication. UV-Vis absorption spectra of $BiCl_3$ solution showed bands at 373 nm and 234 while for bismuth oxide NPs solution, the absorption of Plasmon peak depicts Bi^0 formation by the

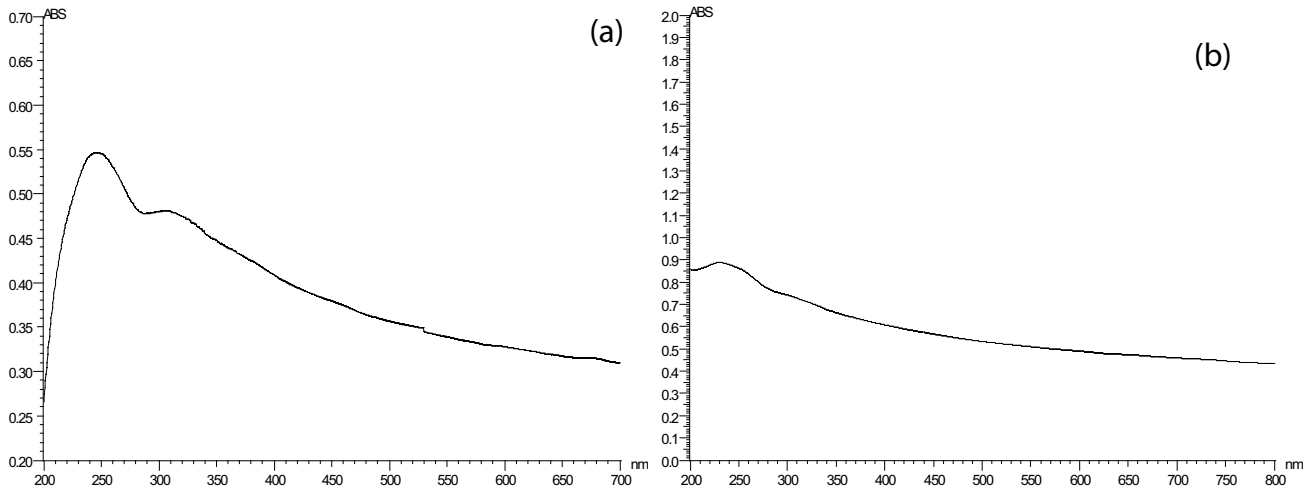

Fig. 3. UV/Vis spectrum of (a) graphene oxide and (b) PM-reduced graphene oxide.

reduction of Bi^{3+} which was apparent due to the presence of plasmon adsorption peak around 397 nm (Fig. 4).

Fourier transform infrared-attenuated total reflectance (FTIR-ATR) spectra were recorded in the range of 375–4,000 cm^{-1}. FTIR spectroscopy is commonly used to provide information on different functional groups in the molecular structure. This technique is valuable for identifying the chemical bonds on the surface of graphene oxide (GO) and rGO. When graphite flakes are oxidized by employing strong oxidizing agents, the carbon atoms layer of graphite is decorated by oxygen-containing groups. These oxygen-containing groups were identified by FTIR spectroscopy. For RGO, some of these absorption peaks are absent or the intensity of them is decreased, which confirms the reduction of graphene oxide.

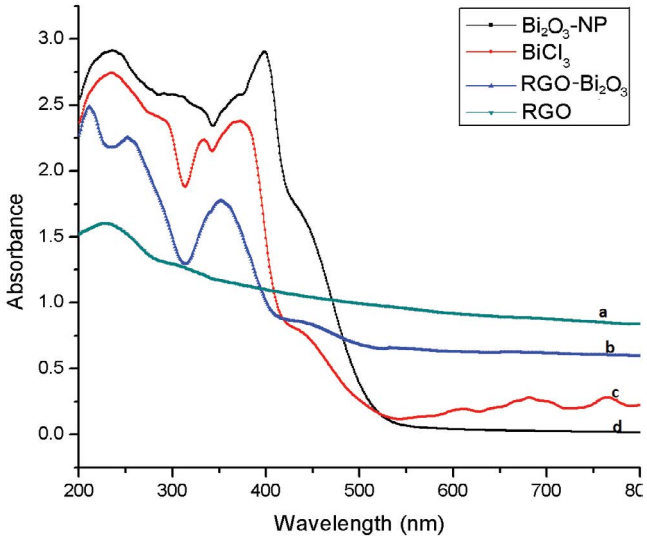

Fig. 4. UV/Vis spectrum of (a) reduced graphene oxide, (b) Bi_2O_3@RGO nanocomposite, (c) aqueous solution of $BiCl_3$ (1 mM), and (d) Bi_2O_3 NPs using 1 mM of $BiCl_3$.

No oxygen-containing functionality was observed in crude graphite powder but after the oxidation, the oxide of graphite is produced with several oxygen-containing functional groups like OH, COOH, epoxy, etc., as depicted in Fig. 5. These functional groups were identified as O–H stretching vibration (3,167 cm^{-1}); C=O stretching vibration and C=C from un-oxidized sp^2 C–C bonds at (1,718 and 1,605 cm^{-1}); C–OH stretching (1,161 cm^{-1}) and C–O vibrations (~855 and 829 cm^{-1}). After the reduction process, these functional groups reduced significantly as is evident from Fig. 5. In ATR spectra of Bi_2O_3@RGO nanocomposite (Figs. 6a and b), the intensity of oxygenated peaks is decreased more indicating a further reduction of GO. Along with reduction, a peak shift of C=O from 1,712 in RGO to 1,625 in nanocomposite was observed indicating attachment of metal on the surface of RGO sheets. The vibrational frequencies of metal-oxygen bond appear in the range of ~375–600 cm^{-1}, peaks ~490–500 cm^{-1} are assigned to Bi–O bond stretching whereas peaks in the range of ~826; 1,027; and 1,399 cm^{-1} are supposed to assign to of Bi–O bond bending vibration and bond of bismuth oxide with oxygen functionalities of RGO [29,30].

The XRD analysis of RGO and Bi_2O_3@RGO nanocomposite is shown in Figs. 7a and b, respectively. In Fig. 7a, peak at $2\theta = 9.8°$ is showing presence of graphene oxide and a broad shoulder at $2\theta = 22.8°$ due to reduced GO. For the Bi_2O_3@RGO (Fig. 7b), peaks correspond to that of monoclinic α-Bi_2O_3 [19]. Average particle size was calculated 12 nm by Scherer's formula, that is:

$$d = \frac{K\lambda}{\beta\cos\theta} \tag{1}$$

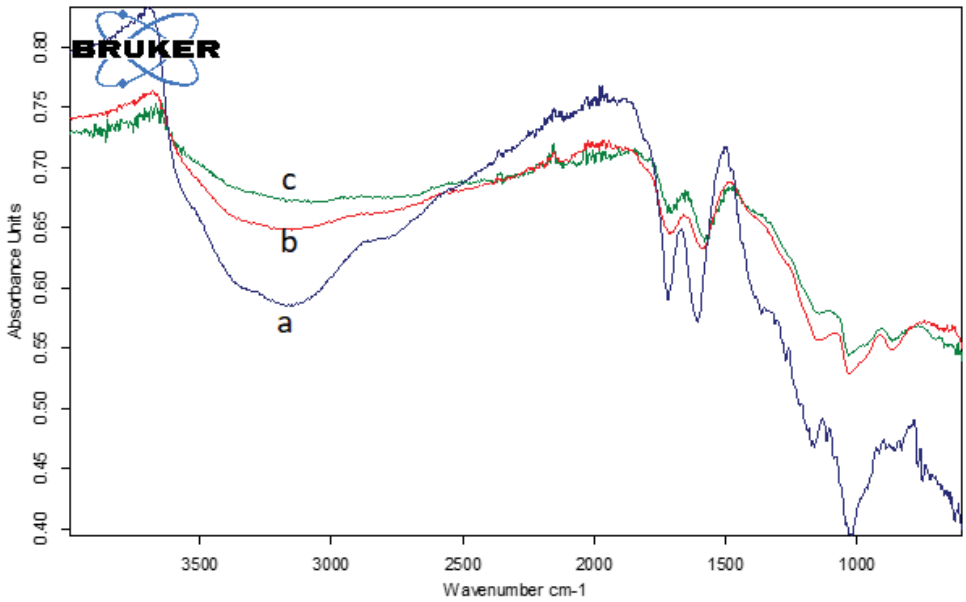

Fig. 5. ATR-FTIR spectra of (a) graphite oxide, (b) graphene oxide, and (c) reduced graphene oxide.

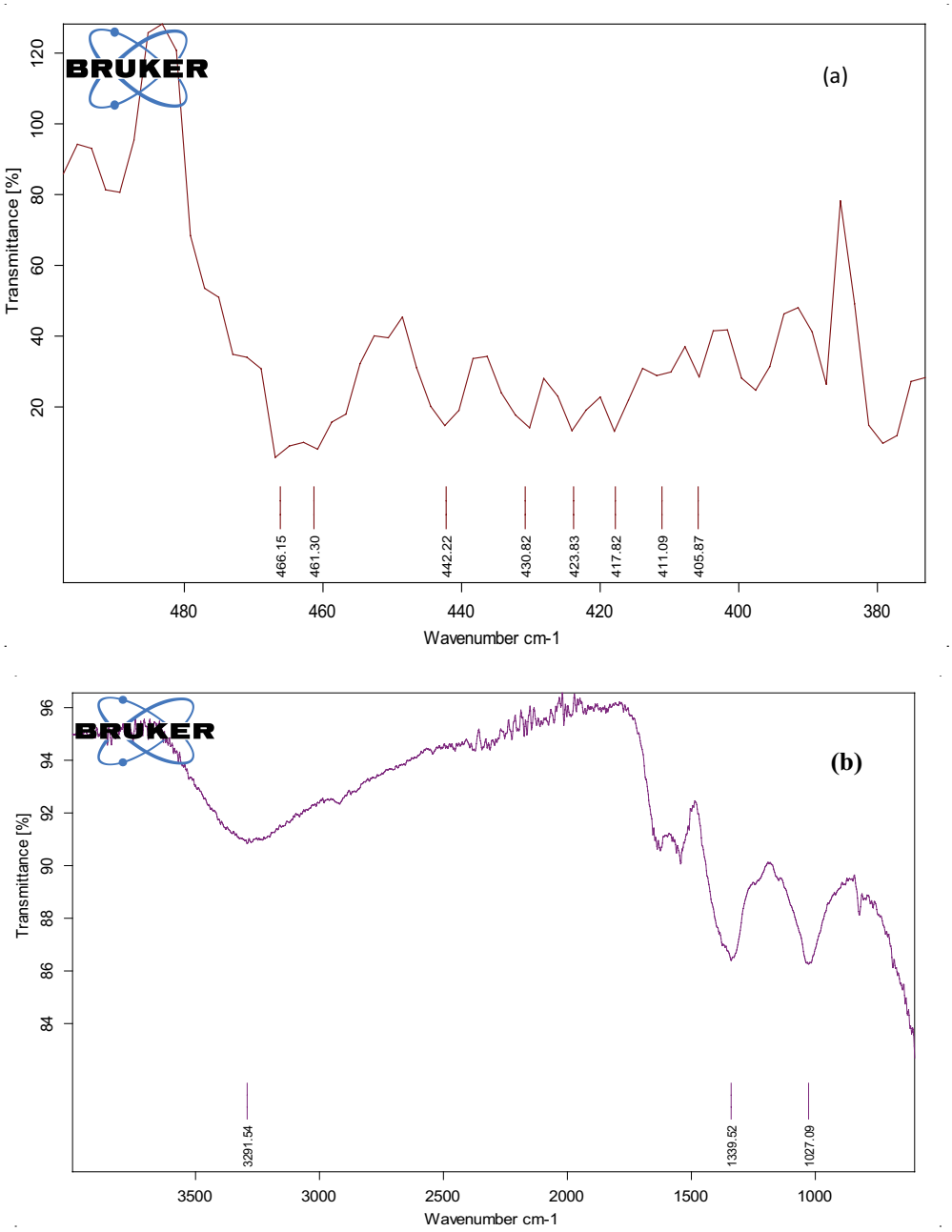

Fig. 6. (a and b) ATR-FTIR spectra of Bi_2O_3@reduced graphene oxide nanocomposite.

where *d* is the depth of crystallite, *K* is the constant reliant on crystallite shape, λ is the incident X-ray wavelength, *B* is the full width at half maximum, θ is the diffracted angle. Partial reduction of graphene oxide is also confirmed by XRD analysis.

4. Photocatalytic activity of Bi_2O_3@RGO nanocomposite

The photocatalytic ability of prepared nanocomposite was assessed by determining the photodecomposition of different dyes like Alizarin yellow, Methylene blue, and Lissamine green. For this purpose, conditions were optimized for concentration of catalyst to be used for the experiments taking Lissamin green as model pollutant. After maintaining equilibrium, experiments were conducted by using increasing amount of catalyst, that is, 5, 10, 15, 20, 25, 30, and 35 mg of catalyst, keeping all other parameters constant. An increase in % photodegradation efficiency was observed with increasing concentration upto 25 mg after which no significant change was observed (Fig. 8). All other photodegradation experiments were conducted by using 25 mg of catalyst.

To predict photodegradative potential of prepared material, an aqueous solution of individual dye along with the catalysts (RGO- and Bi_2O_3@RGO nanocomposites in different experiments) was placed in dark (absence

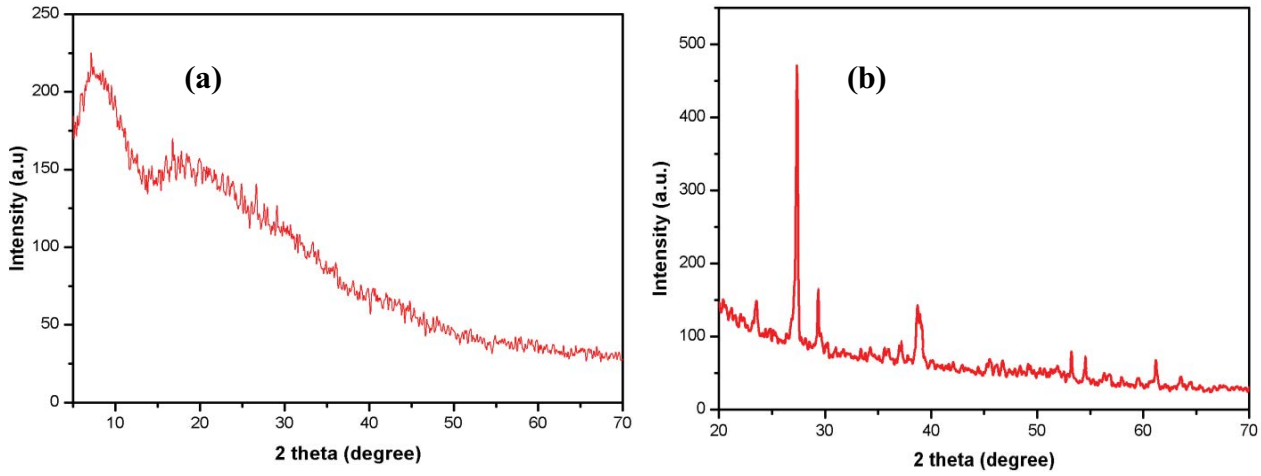

Fig. 7. XRD patterns of (a) RGO and (b) Bi_2O_3@RGO nanocomposite.

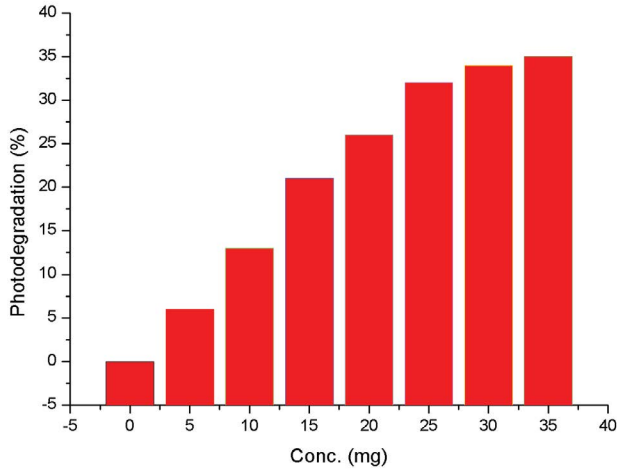

Fig. 8. Optimization of photocatalytic degradation of Lissamine green by using 5, 10, 15, 20, 25, 30, and 35 mg Bi_2O_3@RGO.

of sunlight) so as to ensure the establishment of adsorption/desorption equilibrium. Afterwards the mixture was placed under the sunlight for photocatalytic degradation. The absorbance of the mixture was determined after half an hour by UV-vis spectrophotometer. Afterwards the reaction mixture was again kept in the daylight for 2 h with unceasing stirring, so to determine the photocatalytic degradation of the dyes. Progress in the degradation of the dyes was determined by taking the UV spectrum after fix intervals of the time.

For Lissamine green, similar experiment was executed with 1.0 ppm aqueous solution of dye, 25 mg of nanocomposite as the photocatalytic degradation material in different experimentation. The experiment was performed in intense sunlight at 11:00 a.m. to 2:00 p.m. The adsorption–desorption equilibrium of the dyes was allowed to establish in the dark before the execution of the experiment and the dark adsorption values were recorded. Subsequently, the mix along with the catalyst was placed in daylight with unceasing stirring. The dye absorbance was determined to be 664 nm via UV-Vis spectrophotometer after every 15 min for one and half hour (Fig. 9a). The data depicted that with the increase amount of catalyst there is increased degradation of the dyes. The photocatalytic efficiency of nanocomposites was determined by devising the graph between time period and % dye removal (Fig. 9b). The % degradation of the dyes was determined from following relation:

$$\frac{\text{Initial absorbance} - \text{Final absorbance}}{\text{Initial absorbance}} \quad (2)$$

Concentrations and the absorbance were found to be varying directly with each other, so the results were determined relative to the concentrations. Catalyst was the cause of degradation of the dye, as there is no decline in the concentration of the dye in the solution without catalyst (blank).

For Alizarin yellow GG, the experiment was conducted with a dilute solution of the dye and the 25 mg of the catalyst under the previously described conditions. The dye showed maximum absorbance at 372 nm. The absorbance of the dye was noted after every 15 min for the total period of 90 min (Fig. 10a). The photocatalytic ability of the nanocomposite was determined by developing the graph time and the percentage dye removal (Fig. 10b).

Similar experiment was adopted for degradation of Methylene blue only with different amount of catalyst (25 mg). Spectrophotometric analysis was made at 663 nm (Fig. 11a). Intriguingly better results were achieved for the degradation of MB and the photodegradation was found to be 50% in 90 min (Fig. 11b). Comparative analysis has been made to determine the strength of prepared photocatalyst toward the degradation of MB with respect to already prepared bismuth and graphene oxide-based materials (Table 1). As far as Lissamine green and Alizarin yellow are concerned, no photodegradation studies are reported with prepared nanocomposite, to the best of our knowledge.

The catalyst initiates the decomposition of the dyes in sunlight. Most intriguingly, the light stimulated decomposition of all dyes by Bi_2O_3@RGO nanocomposite was found to be more effectual when compared to decomposition done only by RGO. The mechanism for this photo-degradation

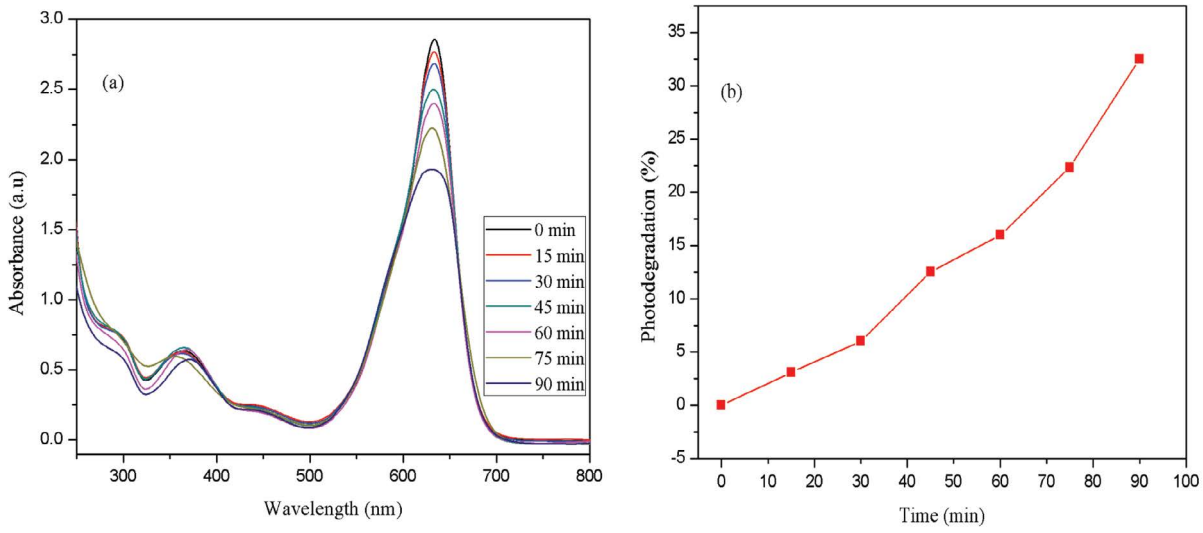

Fig. 9. (a) UV/Vis spectra of photodegradation of Lissamine green via 25 mg PM-Bi_2O_3@RGO nanocomposite and (b) a plot between % photodegradation vs. time (minutes) for photodegradation of Lissamine green.

Table 1
Comparison of photocatalytic degradation of Methylene blue (MB) in aqueous solution by graphene-based Bi_2O_3 nanocomposites with literature

Photo-catalyst	Size/shape of Bi_2O_3 NPs	Amount of photocatalyst (mg)	% degradation of Methylene blue	Reduction time (min)	Reference
PM (*A. javanica)*-Bi_2O_3@RGO	12 nm/spherical	25	52.89	90	Our system
Bi_2O_3-RGO	Needle like	10	98	240	[18]
β-Bi_2O_3/GR	100 nm/oval	500	65	240	[22]
Bi_2O_3-RGO	10–40 nm/cube	2,000	96	240	[31]

involves when dye molecules are exposed to sunlight, the photons strike the nanoparticles in the colloidal mixture and due to this interaction, the electrons at the surface of the particle are excited. These excited electrons (e^-) move from the valence band to conduction band of Bismuth, hence forming holes in valence band resulting in the formation of electron–hole pairs [1]. These electrons, from the nanoparticles surface, transfer promptly to the peripheral area of graphene because of close contact between the RGO surface and Bi_2O_3 nanoparticles, this results in a significantly enhanced active period of the electron–hole pair. Owing to high charge carrier kinesis of graphene, RGO serve as electron transporter and acceptor so as to avert the recombination of photogenerated electron–hole pairs. These electrons are responsible for the conversion of dissolved oxygen molecules of the reacting medium into the oxygen anion radicals. Simultaneously the holes react with the adsorbed water and generate hydroxyl radicals (•OH). These newly generated radicals cause the cleavage of the dye molecules and cause their degradation. The same mechanism was observed in literature [32].

5. Kinetics of photodegradation of dyes

Catalytic activity of Lissamine green, Alizarin yellow, and Methylene blue was investigated by using Bi_2O_3@RGO nanocomposite. Reduction was performed with the assistance of light radiations. Lisamine green, Alizarin yellow, and Methylene blue are UV-vis active and exhibit absorption peaks at 633, 373, and 664 nm, respectively. Hence, photocatalytic degradation was monitored by using ultraviolet-visible spectrophotometry. The typical reduction in peak intensity at 633 nm for Lissamine green, at 373 nm for Alizarin yellow and at 664 nm for Methylene blue was observed in the presence of Bi_2O_3@RGO nanocomposite, which shows that this material exhibit excellent catalytic activity for photocatalytic degradation of dyes.

Photodegradation of Lissamine green, Alizarin yellow, and Methylene blue follows the pseudo-first-order kinetics, because rate of reaction depends upon the concentration of used dye, while sunlight is used in large excess. Pseudo-first-order reaction integrated equation is given as:

$$\ln\frac{C_t}{C_0} = \ln\frac{A_t}{A_0} = -k_{app}t \tag{3}$$

where C_t/C_0 is the ratio of dye concentration at any time t to the concentration of dye at time zero. Concentration of the species is directly related to the absorbance so, this ratio can be replaced by A_t/A_0, at wavelength maxima and

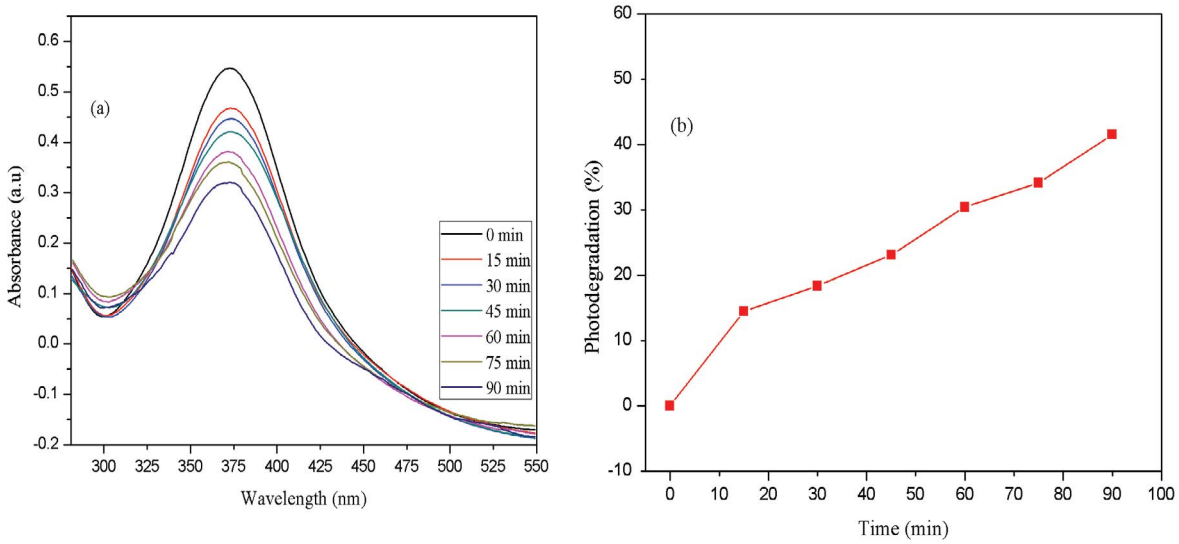

Fig. 10. (a) UV/Vis spectra of photodegradation of Alizarin yellow via 25 mg PM-Bi_2O_3@ RGO nanocomposite and (b) a plot between % photodegradation vs. time (minutes) for photodegradation of Alizarin yellow.

k_{app} is pseudo-first-order evident rate constant for catalytic reduction of dyes. It is obvious from the figure that intensity of absorption peak at wavelength maxima of respective dye by exposure to sun light was decreasing with the passage of time, which shows that dye is degrading with time. Direct photodegradation of dyes was not observed without using catalyst. This observation depicts that the total degradation of the dye mixture is not finished after 1.5 h of the sunlight exposure and the decomposed products of the dye still exists in the solution; hence, for complete eradication of the dye the exposure of the mixture to the sunlight should be increased.

A classic plot of $\ln A_t/A_0$ vs. time is shown in Fig. 12 for photodecomposition of azo dyes. The apparent rate constant was found to be 0.004, 0.005, and 0.007 min^{-1} for Lissamine green, Alizarine yellow, and Methylene blue, respectively. These experimental results show that photocatalytic decomposition of dyes obeys pseudo-first-order reaction. The apparent rate constant value is greater for photodegradation of Methylene blue as compared to Alizarin yellow and Lissamine green which shows that this catalyst is more efficient for photodegradation of Methylene blue (Table 2).

6. Stability of BFO material

Post-structural stability of Bi_2O_3@RGO nanocomposite was investigated by comparing the XRD peak pattern after application in photocatalytic degradation experiment. The XRD peak patterns were found to be similar as obtained before application for photocatalytic degradation

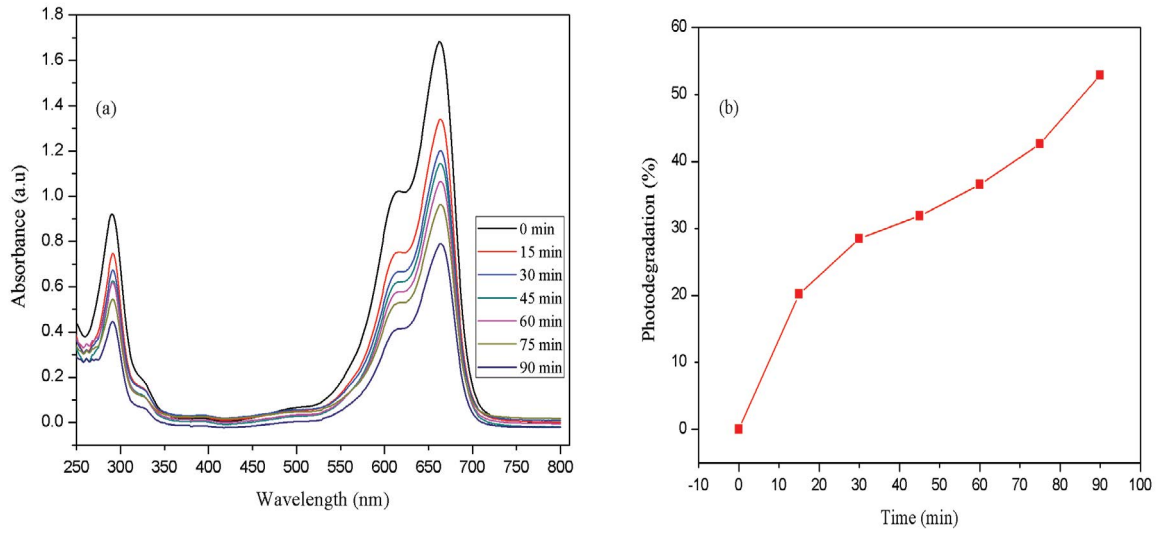

Fig. 11. (a) UV/Vis spectra of photodegradation of Methylene blue via 25 mg PM-Bi_2O_3@ RGO nanocomposite (b) a plots between % photodegradation vs. time (minutes) for photodegradation of Methylene blue.

Table 2
% Photodegradation and apparent rate constant values for catalytic photodegradation of dyes by using 25 mg catalyst dose

Catalyst dose	Dye	% Photodegradation	Apparent rate constant (min^{-1})
25 mg	Lissamine green	32.51	0.004
25 mg	AYGG	41.50	0.005
25 mg	Methylene blue	52.89	0.007

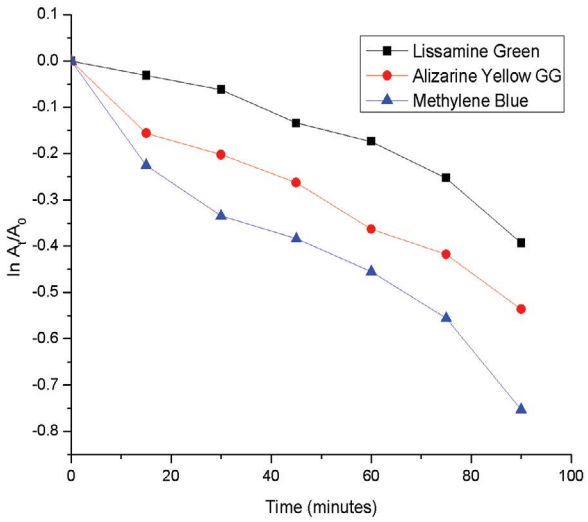

Fig. 12. Values of $\ln(A_t/A_0)$ as a function of time for photodegradation of dyes with 25 mg catalyst dose.

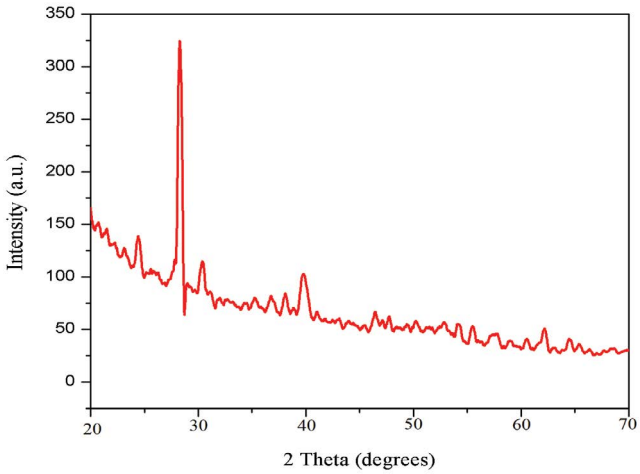

Fig. 13. Post-XRD spectrum for Bi_2O_3@RGO nanocomposite (after photolytic degradation application for Lissamin Green dye).

as shown in Fig. 13. It could be extracted from results that prepared nanocomposite is stable and resistant for any physical and chemical damages during the experiment.

7. Conclusion

In the current study, highly active Bi_2O_3@RGO material was manufactured by a simple green technology, based on the use of aq. extract of flowers of *A. javanica* as a reducing as well as capping agent. UV/Vis and FTIR spectroscopic results, in comparison with reported literature, confirmed the successful synthesis of the final product. The photocatalytic efficiency of the fabricated photocatalytic substances was evaluated for the degradation of industrial dyes under the exposure of sunlight. The results of the photo-decomposition studies showed that the rate of photo-decomposition strongly depends on the radiation exposure and the concentration of catalyst as no degradation were observed in the absence of the catalyst. The results indicated that 25 mg of synthesized material was able to perform 32.51%, 41.50%, and 52.89% degradation of Lissamine green, Alizarin yellow, and Methylene blue, respectively, in 1.5–2 h using sunlight irradiation. The apparent rate constant values for the photocatalytic degradation of Lissamine green, Alizarin yellow, and Methylene blue was found to be 0.004, 0.005, and 0.007 min^{-1}, respectively. PM-RGO/Bi_2O_3 was found more efficient for photocatalytic degradation of Methylene blue as compared to other dyes.

Acknowledgments

The authors are thankful to The Women University Multan for Funding the project.

References

[1] Y.H. Chiu, T.M. Chang, C.Y. Chen, M. Sone, Y.J. Hsu, Mechanistic insights into photodegradation of organic dyes using heterostructure photocatalysts, Catalysts, 9 (2019) 430, doi: 10.3390/catal9050430.
[2] M. Siegrist, M.E. Cousin, H. Kastenholz, A. Wiek, Public acceptance of nanotechnology foods and food packaging: the influence of affect and trust, Appetite, 49 (2007) 459–466.
[3] A. Al Nafiey, A. Addad, B. Sieber, G. Chastanet, A. Barras, S. Szunerits, R. Boukherroub, Reduced graphene oxide decorated with Co_3O_4 nanoparticles (rGO-Co_3O_4) nanocomposite: a reusable catalyst for highly efficient reduction of 4-nitrophenol, and Cr(VI) and dye removal from aqueous solutions, Chem. Eng. J., 322 (2017) 375–384.
[4] W.W. Anku, S.O. Oppong, P.P. Govender, Bismuth-Based Nanoparticles as Photocatalytic Materials, Y. Zhou, F. Dong, S. Jin, Eds., Bismuth – Advanced Applications and Defects Characterization, IntechOpen, 2018, p. 25. Available at: https://www.intechopen.com/books/bismuth-advanced-applications-and-defects-characterization/bismuth-based-nanoparticles-as-photocatalytic-materials
[5] J. Schneider, M. Matsuoka, M. Takeuchi, J. Zhang, Y. Horiuchi, M. Anpo, D.W. Bahnemann, Understanding TiO_2 photocatalysis: mechanisms and materials, Chem. Rev., 114 (2014) 9919–9986.
[6] K. Chakraborty, S. Ibrahim, P. Das, S. Ghosh, T. Pal, Reduced graphene oxide-CdS nanocomposite with enhanced photocatalytic 4-nitrophenol degradation, AIP Conf. Proc., 1832 (2017) 050077, doi: 10.1063/1.4980310.

[7] R. Saravanan, F. Gracia, A. Stephen, Basic Principles, Mechanism, and Challenges of Photocatalysis, M.M. Khan, D. Pradhan, Y. Sohn, Eds., Nanocomposites for Visible Light-Induced Photocatalysis, Springer, Cham, 2017, pp. 19–40.
[8] S.A. Mousavi, M. Hassanpour, M. Salavati-Niasari, H. Safardoust-Hojaghana, M. Hamadanian, Dy_2O_3/CuO nanocomposites: microwave assisted synthesis and investigated photocatalytic properties, J. Mater. Sci. - Mater. Electron., 29 (2018) 1238–1245.
[9] A.H. Al-Marri, M. Khan, S.F. Adil, A. Al-Warthan, W. Tremel, J.P. Labis, M.R.H. Siddiqui, M.N. Tahir, *Pulicaria glutinosa* extract: a toolbox to synthesize highly reduced graphene oxide-silver nanocomposites, Int. J. Mol. Sci., 16 (2015) 1131–1142.
[10] H. Kumar, K. Bhardwaj, K. Kuca, A. Kalia, E. Nepovimova, R. Verma, D. Kumar, Flower-based green synthesis of metallic nanoparticles: applications beyond fragrance, Nanomaterials, 10 (2020) 766, doi: 10.3390/nano10040766.
[11] S. Joseph, B. Mathew, Microwave assisted facile green synthesis of silver and gold nanocatalysts using the leaf extract of *Aerva lanata*, Spectrochim. Acta, Part A, 136 (2015) 1371–1379.
[12] B. Zhang, L. Li, Z. Wang, S. Xie, Y. Zhang, Y. Shen, M. Yu, B. Deng, Q. Huang, C. Fan, Microwave hydrothermal synthesis and photocatalytic properties of TiO_2/$BiVO_4$ composite photocatalysts, Ceram. Int., 39 (2013) 8597–8604.
[13] H. Safardoust-Hojaghana, O. Amirib, M. Salavati-Niasaria, M. Hassanpoura, H. Khojastehc, L.K. Foongd, Performance improvement of dye sensitized solar cells based oncadmium sulfide/S, N co doped carbon dots nanocomposites, J. Mol. Liq., 301 (2020) 112413, doi: 10.1016/j.molliq.2019.112413.
[14] S. Ghasemia, S.J. Hashemiana, A.A. Alamolhoda, I. Gocheva, S.R. Setayesh, Plasmon enhanced photocatalytic activity of Au@TiO_2-graphene nanocomposite under visible light for degradation of pollutants, Mater. Res. Bull., 87 (2017) 40–47.
[15] F. Tavakoli, M. Salavati-Niasari, F. Mohandes, Green synthesis and characterization of graphene nanosheets, Mater. Res. Bull., 63 (2015) 51–57.
[16] M. Mahdiani, F. Soofivand, F. Ansari, M. Salavati-Niasari, Grafting of $CuFe_{12}O_{19}$ nanoparticles on CNT and graphene: eco-friendly synthesis, characterization and photocatalytic activity, J. Cleaner Prod., 176 (2018) 1185–1197.
[17] H. Safardoust-Hojaghan, M. Salavati-Niasari, Degradation of Methylene blue as a pollutant with N-doped graphene quantum dot/titanium dioxide nanocomposite, J. Cleaner Prod., 148 (2017) 31–36.
[18] M. Suresh, A. Sivasamy, Bismuth oxide nanoparticles decorated Graphene layers for the degradation of Methylene blue dye under visible light irradiations and antimicrobial activities, J. Environ. Chem. Eng., 6 (2018) 3745–3756.
[19] T.R. Das, S. Patra, R. Madhuri, P.K. Sharma, Bismuth oxide decorated graphene oxide nanocomposites synthesized via sonochemical assisted hydrothermal method for adsorption of cationic organic dyes, J. Colloid Interface Sci., 509 (2018) 82–93.
[20] S. Zhong, F. Zhang, W. Lu, T. Wang, L. Qua, One-step synthesis of Bi_2WO_6/Bi_2O_3 loaded reduced graphene oxide multicomponent composite with enhanced visible-light photocatalytic activity, RSC Adv., 5 (2015) 68646–68654.
[21] R. Rajagopal, R. Krishnan, A. Ramasubbu, B.A. Kamaludeen, Synthesis of Bi_2WO_6-RGO Nanocomposite for Photocatalytic Application, 2015 International Conference on Smart Sensors and Systems (IC-SSS), Bangalore, 2015.
[22] X. Chen, J. Dai, G. Shi, L. Li, G. Wang, H. Yang, Visible light photocatalytic degradation of dyes by β-Bi_2O_3/graphene nanocomposites, J. Alloys Compd., 649 (2015) 872–877.
[23] M. Du, S. Xiong, T. Wu, D. Zhao, Q. Zhang, Z. Fan, Y. Zeng, F. Ji, Q. He, X. Xu, Preparation of a microspherical silver-reduced graphene oxide-bismuth vanadate composite and evaluation of its photocatalytic activity, Materials, 9 (2016) 160, doi: 10.3390/ma9030160.
[24] S. Mussadiq, N. Riaz, M. Saleem, M. Ashraf, T. Ismail, A. Jabbar, New acylated flavonoid glycosides from flowers of *Aerva javanica*, J. Asian Nat. Prod. Res., 15 (2013) 708–716.
[25] S. Musaddiq, K. Mustafa, S. Ahmad, S. Aslam, B. Ali, S. Khakwani, N. Riaz, M. Saleem, A. Jabbar, Pharmaceutical, ethnopharmacological, phytochemical and synthetic importance of genus *Aerva*: a review, Nat. Prod. Commun., 13 (2018) 375–385.
[26] J. Hummers, S.O. William, E. Richard, Preparation of graphitic oxide, J. Am. Chem. Soc., 80 (1958) 1339–1339.
[27] I. Ali, J.O. Kim, Continuous-flow photocatalytic degradation of organics using modified TiO_2 nanocomposites, Catalysts, 8 (2018) 43, doi: 10.3390/catal8020043.
[28] B. Zhang, L. Li, Z. Wang, S. Xie, Y. Zhang, Y. Shen, M. Yu, B. Deng, Q. Huang, C. Fana, J. Li, Radiation induced reduction: an effective and clean route to synthesize functionalized graphene, J. Mater. Chem., 22 (2012) 7775–7781.
[29] K. Chen, L. Fang, T. Zhang, S.P. Jiang, New zinc and bismuth doped glass sealants with substantially suppressed boron deposition and poisoning for solid oxide fuel cells, J. Mater. Chem. A, 2 (2014) 18655–18665.
[30] M. Ciszewski, A. Mianowski, P. Szatkowski, G. Nawrat, J. Adamek, Reduced graphene oxide–bismuth oxide composite as electrode material for supercapacitors, Ionics, 21 (2015) 557–563.
[31] X. Liu, L. Pan, T. Lv, Z. Sun, C.Q. Sun, Visible light photocatalytic degradation of dyes by bismuth oxide-reduced graphene oxide composites prepared via microwave-assisted method, J. Colloid Interface Sci., 408 (2013) 145–150.